JOURNAL OF MATERIALS SCIENCE **34** (1999) 5127–5132

Kinetic analysis of spinel formation at the interface of CaO-Al_2O_3 fibre-reinforced Al 7075 composites

YUN-MO SUNG*, JAE-WOO AHN
Department of Materials Science and Engineering, Daejin University, Pochun-koon, Kyunggi-do 487-711, South Korea
E-mail: ymsung@road.daejin.ac.kr

A kinetic analysis was performed on the spinel ($MgAl_2O_4$) formation reaction at the interfacial region of the calcium aluminate (CaO-Al_2O_3) fibre-reinforced aluminum 7075 alloy matrix composites (CA/Al 7075) processed at 1200 °K. The counterdiffusion model of Mg^{2+} and Al^{3+} fluxes was employed for the spinel formation reaction. From the parabolic relation between the thickness of the spinel layer and time the reaction rate constant was determined to be a function of the average diffusion coefficient of Al^{3+} ions. By applying the parabolic equation to the experimental data of the CA/Al 7075 the average diffusion coefficient of Al^{3+} ions in the $MgAl_2O_4$ spinel at 1200 °K was calculated and this value appeared to be in small deviation from the extrapolation of previous diffusion coefficient data. *© 1999 Kluwer Academic Publishers*

1. Introduction

The formation of a spinel which can be symbolized in the form of AB_2O_4 is one of the most common and important reactions in ceramics [1–7], ceramic/metal composites [8–11], aluminum alloy melts [12, 13] and so forth. The structure of a spinel can be described as a combined rock salt and zinc blende structure [2]. The oxygen ions have a face-centered cubic close packing. In a unit cell totally 32 oxygen ions, 16 octahedral cations, and 8 tetrahedral cations are involved. For the normal spinel A^{2+} ions occupy tetrahedral sites and B^{3+} ions octahedral sites. The oxides with the spinel structure include $MgAl_2O_4$, $NiAl_2O_4$, $MnAl_2O_4$, $ZnAl_2O_4$, $CoAl_2O_4$, $FeAl_2O_4$, $MgCr_2O_4$, $FeCr_2O_4$, $ZnFe_2O_4$, $CdFe_2O_4$, etc. These spinels show good electronic, magnetic, and high temperature mechanical properties appropriate for industrial applications such as electrolytes, electromagnetic devices and refractories.

Much study has been focused on the formation of $MgAl_2O_4$ spinel [3–5]. By using marker tests Carter [3] proved the counterdiffusion of Mg^{2+} and Al^{3+} ions in the $MgAl_2O_4$ spinel formed between MgO and Al_2O_3. In the spinel layer the markers were found at the one-quarter position from the MgO-$MgAl_2O_4$ interface. Whitney and Stubican [4] obtained the interdiffusion coefficients in $MgAl_2O_4$ spinel in the range of 1833 to 2173 °K. They also found that the interdiffusion coefficient was almost constant according to the composition at 1873 °K. Zhang *et al.* [5] performed diffusion couple tests to study the interdiffusion of MgO and Al_2O_3 and calculated the average diffusion coefficients in the range of 1473 to 1873 °K. Wang and Dudek [10] investigated the $MgAl_2O_4$ spinel formation at the interface of δ-Al_2O_3 fibre reinforced Al-Si-Cu-Mg-Ni alloys using analytical transmission electron microscopy.

Sung [11] fabricated calcium aluminate fibre reinforced aluminum 7075 alloy matrix composites (CA/Al 7075) using the melt infiltration both at 973 and 1200 °K for 2 h. The calcium aluminate (CA) fibres fabricated via inviscid melt spinning (IMS) [14–16] were composed of 46.5 wt % CaO and 53.5 wt % Al_2O_3. The aluminum alloy manufactured by Alcoa Technical Centre (Alcoa Centre, PA, USA) contained alloying elements of 5.6 wt % Zn, 2.5 wt % Mg, 1.6 wt % Cu and 0.23 wt % Cr. The CA/Al 7075 processed at 973 °K showed good interfacial bonding between the CA fibres and the Al 7075 matrix which resulted from the reduced surface tension caused by the accumulation of alloying elements at the interfacial region. The composites processed at 1200 °K showed the formation of a distinct reaction layer with an averaged thickness of $\sim 15\ \mu m$ between the CA fibres and the Al 7075 matrix as well as excellent interfacial bonding. The averaged interfacial thickness value was obtained by investigating 50 fiber-matrix interfacial regions. From the phase and compositional analyses using X-ray diffraction (XRD) and energy dispersive X-ray spectroscopy (EDS) the reaction layer was identified as $MgAl_2O_4$ spinel. The thermodynamic consideration suggested the most probable procedure for the spinel formation. The Mg in the Al 7075 alloy melt firstly oxidized to form the solid MgO, this MgO reacting with Al_2O_3 in the CA fibres to form the $MgAl_2O_4$ spinel. Fig. 1 shows the scanning electron

---

* Author to whom all correspondence should be addressed.

0022–2461

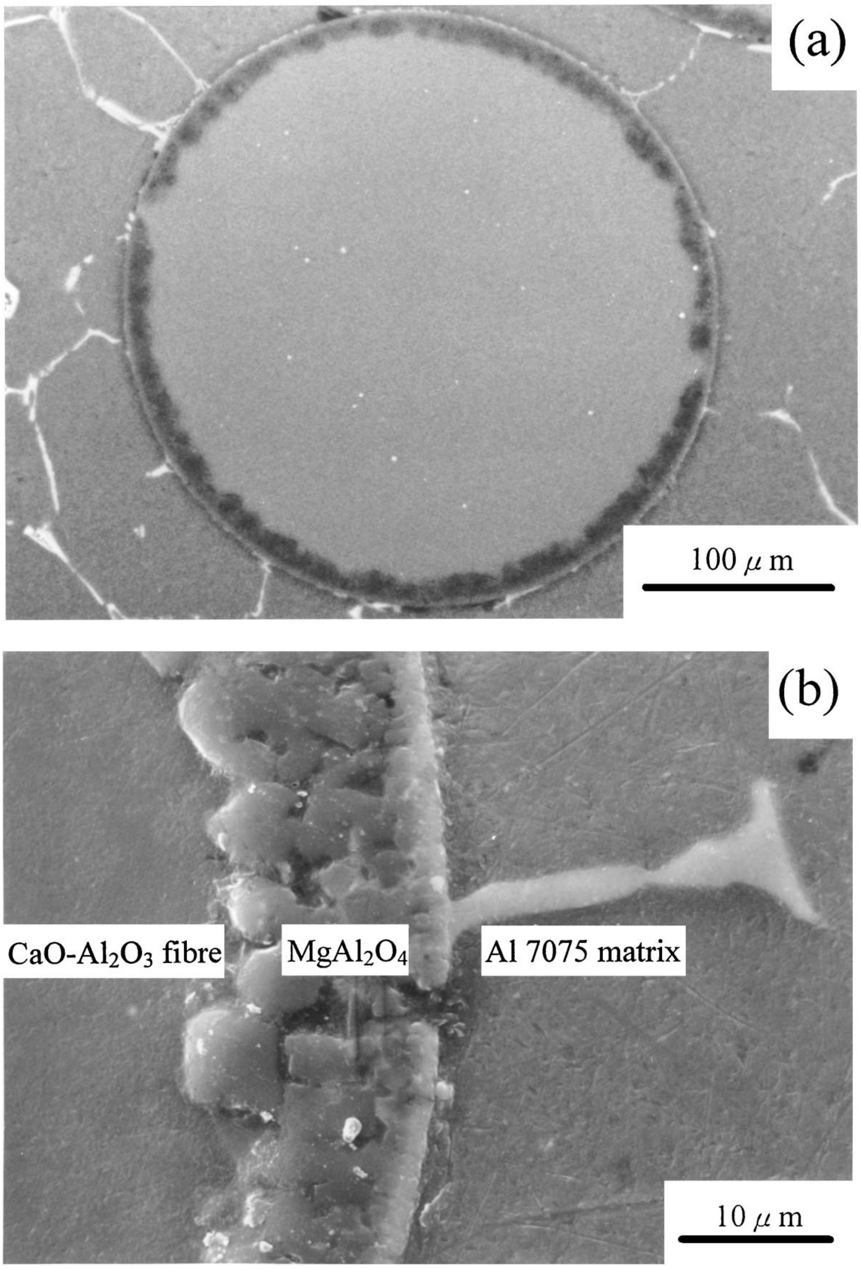

Figure 1 (a) The SEM back scattered electron image (BEI) of the IMS CaO-Al_2O_3 fibre-reinforced Al 7075 alloy composite (CA/Al 7075) processed at 1200 °K for 2 h. (b) The SEM secondary electron image (SEI) of the interfacial region of the corresponding CA/Al 7075. Approximately 15 μm-thick $MgAl_2O_4$ spinel was formed at the interface [11].

micrographs (SEM) of the CA/Al 7075 processed at 1200 °K for 2 h (a) and the blown-up interfacial region of the corresponding composite (b). Approximately 15 μm-thick spinel layer is shown between the CA fibres and matrix.

For present study the kinetics of the spinel formation at the interface of the CA/Al 7075 composites processed at 1200 °K was investigated. The average diffusion coefficient was calculated by employing the parabolic equation to the experimental condition of the spinel formation. This value was compared with the diffusion coefficient data of previous studies [4, 5].

2. Chemistry at the interfaces

The possible mechanism of the $MgAl_2O_4$ spinel formation is the counterdiffusion of the two different cations, Mg^{2+} in MgO and Al^{3+} in Al_2O_3 through the spinel layer [1–5]. Fig. 2 shows the schematic diagrams of the spinel formation. While the reactions at the two interfaces of MgO-$MgAl_2O_4$ and $MgAl_2O_4$-Al_2O_3 can be expressed by using the linear kinetics the transport through the spinel layer by the parabolic kinetics. The spinel formation reaction occurring at the MgO-$MgAl_2O_4$ interface can be expressed as

$$2Al^{3+} + 4MgO \rightarrow 3Mg^{2+} + MgAl_2O_4 \qquad (1)$$

Here, four moles of MgO react with the two moles of Al^{3+} ions to form one mole of $MgAl_2O_4$. The spinel formation reaction at the $MgAl_2O_4$-Al_2O_3 interface can be written as

$$3Mg^{2+} + 4Al_2O_3 \rightarrow 2Al^{3+} + 3MgAl_2O_4 \qquad (2)$$

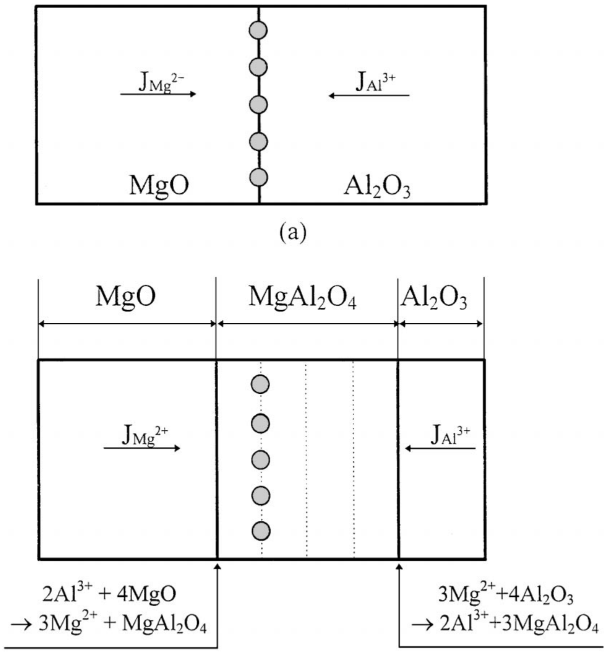

Figure 2 The schematic diagram representing the spinel formation: (a) At the initial stage MgO and Al_2O_3 were contacted with each other and the markers were located at the interface. (b) After time passed at a temperature the $MgAl_2O_4$ spinel was formed between MgO and Al_2O_3. Two types of fluxes, Mg^{2+} and Al^{3+} were counterdiffusing. At the MgO-$MgAl_2O_4$ interface one mole of $MgAl_2O_4$ was formed and at the $MgAl_2O_4$-Al_2O_3 interface three moles of $MgAl_2O_4$. Thus, the markers became located at the one-quarter of the spinel layer from the MgO-$MgAl_2O_4$ interface.

Here, four moles of Al_2O_3 react with three moles of Mg^{2+} ions to form three moles of $MgAl_2O_4$. Combining the Equations 1 and 2 gives

$$\mathrm{MgO} + \mathrm{Al_2O_3} \rightarrow \mathrm{MgAl_2O_4} \tag{3}$$

The three moles of $MgAl_2O_4$ form at the $MgAl_2O_4$-Al_2O_3 interface; one mole of $MgAl_2O_4$ at the MgO-$MgAl_2O_4$ interface. Thus, as shown in Fig. 2 the markers which were originally located at the interface of the MgO-Al_2O_3 shifted to the one-quarter position of the spinel layer from the MgO-$MgAl_2O_4$ interface.

3. Flux equations of the two cations

For the spinel formation reaction not only the chemical potential but also the electrical potential must be included in each flux equation since the diffusing species are the electrically charged cations, Mg^{2+} and Al^{3+}. The electrochemical potential considered as a driving force for the diffusion reaction can be written as following [1, 2]:

$$\eta_i = \mu_i + z_i F\phi \tag{4}$$

where η_i is the electrochemical potential of an i species; μ_i the chemical potential; z_i the valence; F the Faraday constant; ϕ the electrical potential.

The fluxes of Mg^{2+} and Al^{3+} ions were taken into account as following:

$$J_{\mathrm{Mg}^{2+}} = -\frac{C_{\mathrm{Mg}^{2+}} D_{\mathrm{Mg}^{2+}}}{RT}\left[\frac{d\mu_{\mathrm{Mg}^{2+}}}{d\xi} + zF\frac{d\phi}{d\xi}\right] \tag{5}$$

$$J_{\mathrm{Al}^{3+}} = -\frac{C_{\mathrm{Al}^{3+}} D_{\mathrm{Al}^{3+}}}{RT}\left[\frac{d\mu_{\mathrm{Al}^{3+}}}{d\xi} + zF\frac{d\phi}{d\xi}\right] \tag{6}$$

Here, $C_{\mathrm{Mg}^{2+}}$ and $C_{\mathrm{Al}^{3+}}$ are the concentrations of Mg^{2+} and Al^{3+} ions; $D_{\mathrm{Mg}^{2+}}$ and $D_{\mathrm{Al}^{3+}}$ the diffusion coefficients; $\mu_{\mathrm{Mg}^{2+}}$ and $\mu_{\mathrm{Al}^{3+}}$ the chemical potentials; F the Faraday constant; ξ the diffusion distance from the interfaces; z the valence of each species and $+2$ and $+3$ for the Mg^{2+} and Al^{3+} ions, respectively. We assume the oxygen flux is negligible ($J_{\mathrm{O}^{2-}} \approx 0$) relative to the other fluxes of Mg^{2+} and Al^{3+} ions since $D_{\mathrm{Mg}^{2+}}$, $D_{\mathrm{Al}^{3+}} \gg D_{\mathrm{O}^{2-}}$.

The next step is to apply the charge neutrality condition to the two fluxes as following:

$$\sum Z_i J_i = 0\colon 2\, J_{\mathrm{Mg}^{2+}} + 3J_{\mathrm{Al}^{3+}} = 0 \tag{7}$$

Here, by substituting the Equations 5 and 6 into 7 the term of $Fd\phi$ can be solved as

$$Fd\phi = -\left[\frac{2C_{\mathrm{Mg}^{2+}} D_{\mathrm{Mg}^{2+}} d\mu_{\mathrm{Mg}^{2+}} + 3C_{\mathrm{Al}^{3+}} D_{\mathrm{Al}^{3+}} d\mu_{\mathrm{Al}^{3+}}}{4C_{\mathrm{Mg}^{2+}} D_{\mathrm{Mg}^{2+}} + 9C_{\mathrm{Al}^{3+}} D_{\mathrm{Al}^{3+}}}\right] \tag{8}$$

By substituting the Equation 8 into 5 the flux equation can be rewritten as

$$\begin{aligned} J_{\mathrm{Mg}^{2+}} &= -\frac{C_{\mathrm{Mg}^{2+}} D_{\mathrm{Mg}^{2+}} C_{\mathrm{Al}^{3+}} D_{\mathrm{Al}^{3+}}}{RT\left(4C_{\mathrm{Mg}^{2+}} D_{\mathrm{Mg}^{2+}} + 9C_{\mathrm{Al}^{3+}} D_{\mathrm{Al}^{3+}}\right)} \times \left[9\frac{d\mu_{\mathrm{Mg}^{2+}}}{d\xi} - 6\frac{d\mu_{\mathrm{Al}^{3+}}}{d\xi}\right] \\ &= -\frac{C_{\mathrm{Mg}^{2+}} D_{\mathrm{Mg}^{2+}} C_{\mathrm{Al}^{3+}} D_{\mathrm{Al}^{3+}}}{RT\left(4C_{\mathrm{Mg}^{2+}} D_{\mathrm{Mg}^{2+}} + 9C_{\mathrm{Al}^{3+}} D_{\mathrm{Al}^{3+}}\right)} \times \left[\left(9\frac{d\mu_{\mathrm{Mg}^{2+}}}{d\xi} + 9\frac{d\mu_{\mathrm{O}^{2-}}}{d\xi}\right) - \left(6\frac{d\mu_{\mathrm{Al}^{3+}}}{d\xi} + 9\frac{d\mu_{\mathrm{O}^{2-}}}{d\xi}\right)\right] \\ &= -\frac{C_{\mathrm{Mg}^{2+}} D_{\mathrm{Mg}^{2+}} C_{\mathrm{Al}^{3+}} D_{\mathrm{Al}^{3+}}}{RT\left(4C_{\mathrm{Mg}^{2+}} D_{\mathrm{Mg}^{2+}} + 9C_{\mathrm{Al}^{3+}} D_{\mathrm{Al}^{3+}}\right)} \times \left[9\frac{d\mu_{\mathrm{MgO}}}{d\xi} - 3\frac{d\mu_{\mathrm{Al_2O_3}}}{d\xi}\right] \end{aligned} \tag{9}$$

The chemical potentials in the Equation 3 can be written as

$$\mu_{\mathrm{MgO}} + \mu_{\mathrm{Al_2O_3}} = \mu_{\mathrm{MgAl_2O_4}} \approx \mu^{\mathrm{o}}_{\mathrm{MgAl_2O_4}} \tag{10}$$

Here, the chemical potential of the spinel formed between the oxides can be approximated to that of the pure spinel since the concentrations of Mg^{2+} and Al^{3+} ions diffusing through the spinel are extremely low. Differentiating Equation 10 by ξ gives

$$d\mu_{Al_2O_3} = -d\mu_{MgO} \tag{11}$$

Substituting the Equation 11 into 9 gives

$$J_{Mg^{2+}} = -\frac{12C_{Mg^{2+}}D_{Mg^{2+}}C_{Al^{3+}}D_{Al^{3+}}}{RT\left(4C_{Mg^{2+}}D_{Mg^{2+}} + 9C_{Al^{3+}}D_{Al^{3+}}\right)} \times \left[\frac{d\mu_{MgO}}{d\xi}\right] \tag{12}$$

Here, we assume that in the spinel formed between the oxides div $J_{Mg^{2+}} \approx 0$ with the small range of homogeneity. Thus, separating variables and integrating Equation 12 by ξ gives

$$\int_0^{\Delta\xi} J_{Mg^{2+}}d\xi = J_{Mg^{2+}}\Delta\xi = \int_{\mu_{MgO}(MgO - MgAl_2O_4)}^{\mu_{MgO}(Al_2O_3 - MgAl_2O_4)} \frac{12C_{Mg^{2+}}D_{Mg^{2+}}C_{Al^{3+}}D_{Al^{3+}}}{RT\left(4C_{Mg^{2+}}D_{Mg^{2+}} + 9C_{Al^{3+}}D_{Al^{3+}}\right)} d\mu_{MgO} \tag{13}$$

Fig. 3 shows the chemical potential of MgO in the MgO-$MgAl_2O_4$-Al_2O_3 system. As shown, it is a constant value of μ^o_{MgO} inside the MgO and decreases through the $MgAl_2O_4$. It becomes a decreased and constant value of μ_{MgO} in the Al_2O_3. The difference between μ_{MgO} and μ^o_{MgO} is $\Delta\mu_{MgO}$. The reaction equilibrium constant, K can be written as

$$K = \frac{a_{MgAl_2O_4}}{a_{MgO}a_{Al_2O_3}} = \exp\left(-\frac{\Delta G^o_{MgAl_2O_4}}{RT}\right) \tag{14}$$

where $a_{MgAl_2O_4}$, a_{MgO} and $a_{Al_2O_3}$ are the activities of $MgAl_2O_4$, MgO and Al_2O_3, respectively; $\Delta G^o_{MgAl_2O_4}$ the formation free energy of the $MgAl_2O_4$ spinel. At the $MgAl_2O_4$-Al_2O_3 interface $a_{MgAl_2O_4}$ and $a_{Al_2O_3}$ would be approximated to 1. Thus, the Equation 14 can be reduced to $a_{MgO} = \exp(-\frac{\Delta G^o_{MgAl_2O_4}}{RT})$. By definition the chemical potential of MgO can be written as

$$\mu_{MgO} = \mu^o_{MgO} + RT\ln a_{MgO} = \mu^o_{MgO} + \Delta G^o_{MgAl_2O_4} \tag{15}$$

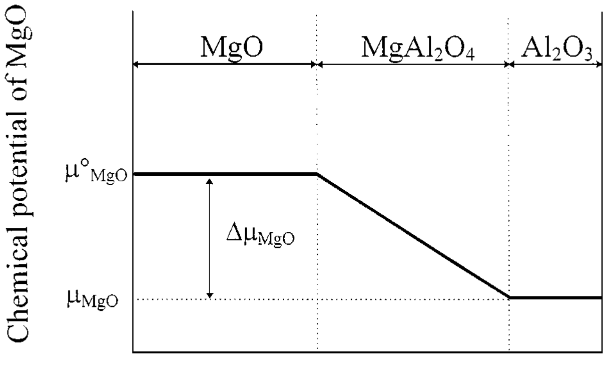

Figure 3 The schematic diagram of the chemical potential of MgO in the MgO-$MgAl_2O_4$-Al_2O_3 system. It is a constant value of μ^o_{MgO} in MgO, decreasing in the $MgAl_2O_4$ layer to be another constant value of μ_{MgO} in the Al_2O_3.

Substituting Equation 15 into 13 gives

$$J_{Mg^{2+}}\Delta\xi = -\frac{12}{RT} \times \int_{\mu^o_{MgO}}^{\mu^o_{MgO} + \Delta G^o_{MgAl_2O_4}} \frac{C_{Mg^{2+}}D_{Mg^{2+}}C_{Al^{3+}}D_{Al^{3+}}}{\left(4C_{Mg^{2+}}D_{Mg^{2+}} + 9C_{Al^{3+}}D_{Al^{3+}}\right)} d\mu_{MgO}$$
$$= -\frac{12}{RT} \times \int_{\mu^o_{MgO}}^{\mu^o_{MgO} + \Delta G^o_{MgAl_2O_4}} \frac{D_{Mg^{2+}}C_{Al^{3+}}D_{Al^{3+}}}{\left(4D_{Mg^{2+}} + 9\frac{C_{Al^{3+}}}{C_{Mg^{2+}}}D_{Al^{3+}}\right)} d\mu_{MgO} \tag{16}$$

Here, $C_{Al^{3+}}$ is a constant and $C_{Al^{3+}}/C_{Mg^{2+}}$ in the $MgAl_2O_4$ spinel is 2. The Equation 16 can be rewritten as

$$J_{Mg^{2+}}\Delta\xi = -\frac{6C_{Al^{3+}}}{RT} \times \int_{\mu^o_{MgO}}^{\mu^o_{MgO}+\Delta G^o_{MgAl_2O_4}} \frac{D_{Mg^{2+}}D_{Al^{3+}}}{\left(2D_{Mg^{2+}} + 9D_{Al^{3+}}\right)} d\mu_{MgO} \tag{17}$$

Here, the term of $D_{Mg^{2+}}D_{Al^{3+}}/(2D_{Mg^{2+}} + 9D_{Al^{3+}})$ is in the form of Nernst-Planck equation. Thus, assuming $D_{Mg^{2+}} \gg D_{Al^{3+}}$ gives $D_{Mg^{2+}}D_{Al^{3+}}/(2D_{Mg^{2+}} + 9D_{Al^{3+}}) \approx D_{Al^{3+}}/2$. By using this relationship the flux equation in the final form can be written as

$$J_{Mg^{2+}}\Delta\xi \approx -\frac{3C_{Al^{3+}}}{RT}\int_{\mu^o_{MgO}}^{\mu^o_{MgO}+\Delta G^o_{MgAl_2O_4}} D_{Al^{3+}}d\mu_{MgO}$$
$$J_{Mg^{2+}} \approx -\frac{3C_{Al^{3+}}\bar{D}_{Al^{3+}}}{\Delta\xi}\left(\frac{\Delta\mu_{MgO}}{RT}\right) \tag{18}$$

where $\bar{D}_{Al^{3+}} = \frac{1}{\Delta\mu_{MgO}}\int_{\mu^o_{MgO}}^{\mu^o_{MgO}+\Delta G^o_{MgAl_2O_4}} D_{Al^{3+}}d\mu_{MgO}$ and can be defined as an average diffusivity of Al^{3+} ions.

4. Kinetics of spinel formation

The growth rate of the $MgAl_2O_4$ spinel can be expressed as

$$\frac{d\Delta\xi}{dt} \equiv \text{Flux} \times \text{Molar volume} \tag{19}$$

From the Equations 1 and 2 the motion of three moles of Mg^{2+} ions gives four moles of spinel. This relationship was schematically drawn in Fig. 2. The growth rate can be written as

$$\begin{aligned}\frac{d\Delta\xi}{dt} &= J_{Mg^{2+}} \times \frac{4}{3}V^{m}_{MgAl_2O_4}\\ &= -\frac{3C_{Al^{3+}}\bar{D}_{Al^{3+}}}{\Delta\xi}\left(\frac{\Delta\mu_{MgO}}{RT}\right)\times\left(\frac{4}{3}V^{m}_{MgAl_2O_4}\right)\end{aligned} \tag{20}$$

Here, $\Delta\mu_{MgO} = \mu_{MgO} - \mu^{o}_{MgO} = (\mu^{o}_{MgO} + \Delta G^{o}_{MgAl_2O_4}) - \mu^{o}_{MgO} = \Delta G^{o}_{MgAl_2O_4}$; $C_{Al^{3+}} = X_{Al^{3+}}/V^{m}_{MgAl_2O_4} = 2/V^{m}_{MgAl_2O_4}$. Thus, substituting these relationships into the Equation 20 and separating variables gives

$$\Delta\xi d\Delta\xi = \bar{D}_{Al^{3+}}\frac{\Delta G^{o}_{MgAl_2O_4}}{RT}dt \tag{21}$$

Integrating the Equation 21 gives

$$\Delta\xi^2 = 2\left(-8\bar{D}_{Al^{3+}}\frac{\Delta G^{o}_{MgAl_2O_4}}{RT}\right)t = 2kt \tag{22}$$

Therefore, the reaction rate constant, k can be defined as

$$k = -8\bar{D}_{Al^{3+}}\frac{\Delta G^{o}_{MgAl_2O_4}}{RT} \tag{23}$$

Thus, the rate of the spinel formation reaction was found to be determined by the average diffusion coefficient of the slower cation, Al^{3+} rather than the faster cation Mg^{2+}.

5. Discussion

From Sung's result [11] the average thickness of the spinel formed at the interacial region of the CA/Al 7075 composites processed at 1200 °K for 2 h was 15 μm. Thus, by substituting these values into the Equation 22 the reaction rate constant, k at 1200 °K was determined as 1.5625×10^{-10} cm^2/s. Also, by substituting the values of k (1.5625×10^{-10} cm^2/s), $\Delta G^{o}_{MgAl_2O_4}$ (−1804 kJ/mol) and T(1200 °K) into the Equation 23 $\bar{D}_{Al^{3+}}$, the average diffusion coefficient of Al^{3+} was calculated as 1.08×10^{-13} cm^2/s.

This value was compared with the diffusion coefficient data of Whitney and Stubican [4], and Zhang *et al.* [5]. Fig. 4 shows the curve fitted based on their data and extrapolated to the lower temperature region. The diffusion coefficient value obtained in present study was marked as x and found to be somewhat higher than that estimated from the extrapolated curve. Approximation from the curve gave the diffusion coefficient value of $\sim 1.56 \times 10^{-14}$ cm^2/s at 1200 °K. The difference between this estimated value and that obtained from present study would be caused by different experimental conditions. As for the solid state diffusion experiments the true contact area at the interface between MgO and Al_2O_3 is much smaller than the sample area due to the surface roughness. Even fine final polishing cannot give a really smooth surface on the atomic scale. Thus, as for the diffusion couple experiments the thickness ($\Delta\xi$) of the spinel would be rather smaller than that of the present study, thus the diffusion coefficient value becomes smaller. As for the solid-liquid reaction in the present study the contact area at the fibre-matrix interface can be maximized before the spinel formation reacion initiates. This is due to the lowered surface tension of the molten Al-Mg alloy, which was caused by the accumulation of the solute atom, Mg at the interface. Moreover, the diffusion of the ions becomes very fast due to a low activation energy for the diffusion resulting from the week bonding between the ions in the Al alloy melt.

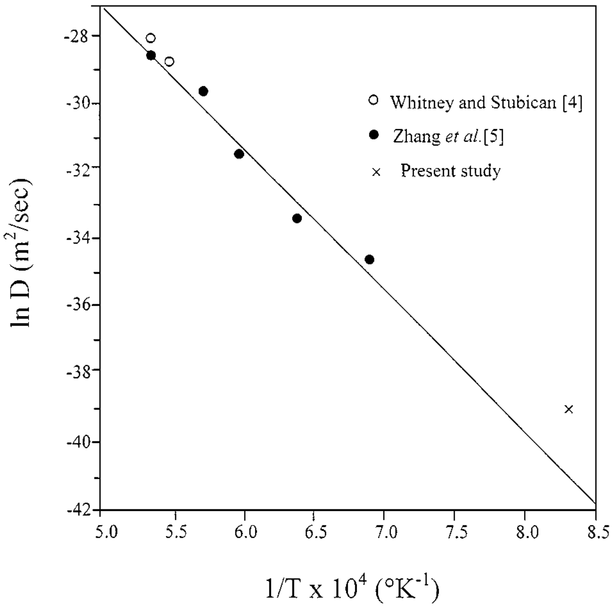

Figure 4 The diagram of average diffusion coefficients in $MgAl_2O_4$ spinel. The curve fitted based on the data of Whitney and Stubican [4] and Zhang *et al.* [5] was extrapolated to the lower temperature range. The average diffusion coefficient obtained in present study was marked as x in the diagram and showed small deviation from the curve.

6. Summary

The $MgAl_2O_4$ spinel formation at the interface of the CA/Al 7075 composites processed at 1200 °K was studied using the kinetic analysis. The diffusion mechanism employed was the counterdiffusion of Mg^{2+} and Al^{3+} ions across the spinel formed between MgO and Al_2O_3. The motion of three moles of Mg^{2+} and two moles of Al^{3+} ions formed totally four moles of $MgAl_2O_4$ spinel. The flux equation was derived in the form: $J_{Mg^{2+}} \approx -\frac{3C_{Al^{3+}}\bar{D}_{Al^{3+}}}{\Delta\xi}(\frac{\Delta\mu_{MgO}}{RT})$. By using the growth rate of the $MgAl_2O_4$ the parabolic equation was obtained as: $\Delta\xi^2 = 2(-8\bar{D}_{Al^{3+}}\frac{\Delta G^{o}_{MgAl_2O_4)}}{RT})t = 2kt$. Therefore, the reaction rate constant, k was a function of the average diffusion coefficient of the slower migrating species, Al^{3+}. By employing the equation to the experimental data the average diffusion coefficient of Al^{3+} at 1200 °K was calculated as 1.08×10^{-13} cm^2/s and it was found to be one-order higher than that (1.56×10^{-14} cm^2/s) estimated from the extrapolation of the previous data. This difference would be caused by the maximized contact area at the fibre-matrix interface and fast diffusion rate of the ions in the Al alloy melt.

Acknowledgement

This study was partially supported by the Daejin University research grants in 1997.

References

1. H. SCHMALZRIED, "Solid State Reactions" (Verlag Chemie, Weinheim, 1981) pp. 105.
2. W. D. KINGERY, H. K. BOWEN and D. R. UHLMANN, "Introduction to Ceramics," Vol. 64 (John Wiley and Sons, New York 1976) pp. 381.
3. R. E. CARTER, *J. Amer. Ceram. Soc.* **44** (1961) 116.
4. W. P. WHITNEY II and V. S. STUBICAN, *J. Phys. Chem. Solids* **32** (1971) 305.
5. P. ZHANG, J. KARWAN-BACZEWSKA, S. DU and S. SEETHARAMAN, *Metall. Mater. Trans. A* **27A** (1996) 2978.
6. P. H. BOLT, S. F. LOBNER, J. W. GEUS and F. H. P. M. HABRAKEN, *Applied Surface Science* **89** (1995) 339.
7. E. ANTOLINI, *Mater. Res. Bull.* **32** (1979) 9.
8. C.-F. HONG, S.-J. LIN and K.-S. LIU, *Mater. Sci. & Eng. A* **A150** (1992) 289.
9. X. SUN and J. YEOMANS, *J. Amer. Ceram. Soc.* **79** (1996) 2705.
10. S. WANG and H. J. DUDEK, *Mater. Sci. & Eng. A* **A205** (1996) 180.
11. Y.-M. SUNG, *J. Mater. Sci.* **32** (1997) 1069.
12. L. RAULT, M. ALLIBERT and A. DUBUS, *Mater. Sci. Forum* **217–222** (1996) 165.
13. H. VENUGOPALAN, K. TANKALA and T. DEBROY, *Mater. Sci. & Eng. A* **A210** (1996) 64.
14. Y.-M. SUNG, S. A. DUNN and J. A. KOUTSKY, *Ceram. Inter.* **21** (1995) 169.
15. *Idem., J. Mater. Sci.* **30** (1995) 5995.
16. Y.-M. SUNG and S. A. DUNN, *ibid.* **31** (1996) 4741.

Received 10 October 1997
and accepted 23 March 1999